Polymer Chemistry

Accepted Manuscript

ROYAL SOCIETY OF CHEMISTRY

www.rsc.org/polymers

Cite this: DOI: 10.1039/c0xx00000x

www.rsc.org/xxxxxx

ARTICLE TYPE

Facile synthesis, sequence-tuned thermoresponsive behaviours and reaction-induced reorganization of water-soluble keto-polymers

Xianghua Tang, Jie Han, Zhengguang Zhu, Xinhua Lu, Hong Chen and Yuanli Cai*

Received (in XXX, XXX) Xth XXXXXXXXX 20XX, Accepted Xth XXXXXXXXX 20XX

DOI: 10.1039/b000000x

We report facile synthesis, sequence-tuned thermoresponsive behaviours and reaction-induced reorganization of ketone-based hydrophilic reactive polymers. The well-controlled and living RAFT polymerisation of the commercially-available diacetone acrylamide (DAAM), in methanol media on irradiation with visible light at 25 ^{o}C, leads to the well-defined keto-polymers over a wide degrees of polymerisation of 50~1000 and the block copolymer with poly(*N*,*N*-dimethyl acrylamide) (PDMA). Statistical copolymerisation with DMA gives the gradient copolymers, P(DAAM-*grad*-DMA), whose aqueous solubility can be finely tuned. Binary copolymers that have the tailored structures of PDMA-*b*-P(DAAM-*grad*-DMA) can be achieved *via* one-pot iterative process. The aqueous solutions of P(DAAM-*grad*-DMA) copolymers exhibit typical thermoresponsive behaviours on heating, whose cloud point can be widely tuned from 16 ^{o}C to permanently water-soluble. Adjusting the sequence from *gradient*, *"short-block"-gradient*, *"middle-block"-gradient*, *"long-block"-gradient* to *block* structure can induce the diversity in the dehydration, heating-triggered phase transition, assembly and reaction-induced dynamic reorganization. These water-soluble reactive keto-polymers are thus promising for emerging biological applications on demand in physiological aqueous solution.

Introduction

There has been renewed interest in the reactive polymers in the recent years.[1] These polymers were used as the precursors for the facile synthesis of functionalized polymers having the same chain lengths without tedious synthesis of specific monomers,[2-7] thus provided a versatile platform for the diversely functionalized polymers from a single precursor.[8-14] To satisfy the applications in biological fields,[15,16] the post reaction should be efficient and without harsh conditions or reagents. Typical example is aldehyde-functionalized polymer because it can readily react with primary amines or oximes to release the eco-friendly side product, water. The aldehyde-functionalized polymers were achieved *via* living polymerisation of acetal monomers[17-20] or the direct synthesis[21-30] *via* reversible addition-fragmentation chain transfer (RAFT) polymerisation.[31]

Similarly, ketone can react with primary amines or oximes to release water under the same mechanism as aldehyde. More importantly, ketone is less likely to be oxidized than aldehyde, thus is excellent candidate for biological applications in aqueous media. The robust feature of ketone has been evidenced in recent papers, e.g. peptide conjugates;[32,33] cell surface engineering;[34,35] tumor-specific chemotherapy;[36] the immobilization,[37] labelling[39] and transamination[38] of proteins; polymer-cellulase conjugates;[40] biodegradable polyketoesters;[41] etc. In contrast to the extensive-studied aldehyde-based polymer, the well-defined keto-polymer was less exploited.[42-45] Rizzardo and coworkers[42] reported the first RAFT synthesis of the homo- and block copolymers based on diacetone acrylamide (DAAM). Schlaad and coworkers[43] used this technique for synthesis of 2-(acetoacetoxy)ethyl methacrylate based keto-polymers. This technique was employed for synthesis of ketal-terminated polymers by Bong and coworkers[44]. Davis and coworkers[45] reported the hydrophobic keto-polymers and the amphiphilic block copolymer via RAFT synthesis. Clearly, the keto-polymers that have aqueous solubility tuned on demand are crucial to satisfy as-mentioned specific applications.[32-41]

This paper describes the facile synthesis of well-defined keto-polymers whose aqueous solubility can be tuned on demand. To this end, commercially-available DAAM was polymerized *via* RAFT polymerisation in methanol on irradiation with visible light at 25 ^{o}C.[46,47] The tunable aqueous solubility was achieved *via* the copolymerisation with *N*,*N*-dimethyl acrylamide (DMA). Copolymers having the tailored structures of PDMA-*b*-P(DAAM-*grad*-DMA) were synthesized *via* a one-pot iterative process.[48] Moreover, the effect of the copolymer sequence on dehydration, heating-triggered phase transition, assembly and reaction-induced reorganization were studied using ^{1}H NMR, GPC and dynamic light scattering (DLS).

Experimental

Materials

DAAM that was donated by Hipro Polymer Materials Co. was re-crystallized from ethyl acetate. DMA (J&K Scientific) passed through a basic alumina column; these monomers were stored in refrigerator at -20 °C. *S*-1-ethyl-*S'*-(α,α'-dimethyl-α''-acetic acid) trithiocarbonate (EDMAT) was synthesized according to the literature.[49] (2,4,6-Trimethylbenzoyl)diphenylphosphine oxide (TPO, Runtec) was recrystallized twice from diethyl ether in the dark. O-Benzylhydroxylamine hydrochloride (BHA, J&K Scientific) was used as received. Methanol was refluxed over Mg/I_2; triethylamine (TEA) was reflux over CaH_2; these agents were distilled before use. Deuterium oxide and methanol-d_4 purchased from Sigma-Aldrich, were used as received. Water was deionized to R > 18.2 MΩ cm^{-1} using an AQUELX 5 Millipore system.

Visible Light

A 400 W mercury lamp was employed. JB400 filters were used to cut off ultraviolet light at $\lambda_{em} < 400$ nm and to reduce intensity to a $I_{420nm} = 0.20$ mW cm^{-2}, which corresponds to approximately 5% of solar radiation on a typical cloudless day at noon in May in East China. The light intensity was measured using a UV-A radiometer that was fitted with a $\lambda = 420$ nm detector.

RAFT polymerisation of DAAM monomer

Typically, DAAM (1.69 g, 10.0 mmol), EDMAT (22.4 mg, 0.1 mmol), TPO (8.7 mg, 0.025 mmol) and 1.721 g methanol were added in a 25-mL reaction flask. The flask capped with rubber septa and immersed in a water bath at 25 °C. The solution was purged with argon gas in the dark for 40 min, and then irradiated with visible light. Samples were taken at pre-determined intervals. Reaction was quenched by addition of traces of hydroquinone. Monomer conversions were assessed by ^1H NMR according to Eq. 1, where $I_{5.52}$ is the integrated signal at $\delta = 5.52$ ppm (one of $C\mathbf{H}_2$=CH of DAAM), $I_{2.04}$ is the integrated signals at $\delta = 2.04$ ppm ($CH_2COC\mathbf{H}_3$ of DAAM and the units). Another portion was used for GPC studies on the number-average molecular weight (M_n) and polydispersity index (M_w/M_n) of the polymer.

$$Conversion_{DAAM} = (1 - \frac{3 \times I_{5.52}}{I_{2.04}}) \times 100\% \tag{1}$$

Statistical copolymerisation of DMA and DAAM monomers

Typically, DMA (0.99 g, 10.0 mmol), DAAM (1.69 g, 10.0 mmol), EDMAT (22.4 mg, 0.1 mmol), TPO (8.7 mg, 0.025 mmol) and 2.711 g methanol were added in a 25-mL reaction flask. This flask was capped with rubber septa and immersed in a water bath at 25 °C. The solution was purged with argon gas in the dark for 40 min, and then irradiated with visible light. Samples were taken at predetermined intervals. Reaction was quenched by addition of traces of hydroquinone. Monomer conversions were assessed by ^1H NMR according to Eqs. 1-2, where $I_{5.64}$ is the integrated signal at $\delta = 5.64$ ppm (one of $C\mathbf{H}_2$=CH of DMA), $I_{5.52}$ is the integrated signal at $\delta = 5.52$ ppm (one of $C\mathbf{H}_2$=CH in DAAM), $[DMA]_0/[DAAM]_0$ is the feed molar ratio of DMA to DAAM.

$$Conversion_{DMA} = \left[1 - \frac{[DMA]_0}{[DAAM]_0} \times \frac{I_{5.64}}{I_{5.52}} (1 - Conversion_{DAAM})\right] \times 100\% \tag{2}$$

Synthesis of PDMA-*b*-PDAAM copolymer

Firstly, DMA (2.376 g, 24 mmol), EDMAT (44.8 mg, 0.2 mmol), TPO (17.4 mg, 0.05 mmol) and 2.04 g methanol were added in a 25-mL reaction flask. The flask was capped with rubber septa and immersed in a water bath at 25 °C. The solution was purged with argon gas in the dark for 40 min, and then irradiated with visible light for 120 min. Reaction was quenched by addition of traces of hydroquinone. The polymer was precipitated from diethyl ether. Weight: 1.76; yield: 87%. ^1H NMR: 93% DMA conversion, $DP_{DMA} = 113$; GPC: $M_n = 21.1$ kg mol^{-1}, $M_w/M_n = 1.10$. Secondly, as-synthesized PDMA (1.65 g, 0.175 mmol), DAAM (2.957 g, 17.5 mmol), TPO (15.2 mg, 0.04375 mmol) and 4.623 g methanol were added to a 25 mL reaction flask. The flask was capped with rubber septa and immersed in a water bath at 25 °C. The solution was purged with argon gas in the dark for 40 min, and then irradiated with visible light for 80 min. Reaction was quenched by addition of traces of hydroquinone. The polymer was precipitated from diethyl ether. Weight: 3.96 g; yield: 86%. ^1H NMR: 94% DAAM conversion, $PDMA_{113}$-*b*-$PDAAM_{93}$; GPC: $M_n = 43.8$ kg mol^{-1}, $M_w/M_n = 1.10$.

Synthesis of PDMA-*b*-P(DAAM-*ran*-DMA) copolymer

Typically, DMA (2.376 g, 24 mmol), EDMAT (44.8 mg, 0.2 mmol), TPO (17.4 mg, 0.05 mmol) and 2.438 g methanol were added in a 25-mL reaction flask. The flask was capped with rubber septa and immersed in water bath at 25 °C. The solution was purged with argon gas in the dark for 40 min, and then irradiated with visible light for 18 min. Thereafter, visible light was turned off. Samples were taken out right after turning off visible light and after keeping in the dark for 20 min. ^1H NMR studies indicated that monomer conversions were both at 31% in between the dark period. The argon-gas-saturated DAAM (3.38 g DAAM in 3.38 g methanol, 20 mmol) was added in the solution in the dark, and then irradiated with visible light at 25 °C for 90 min. ^1H NMR studies indicated that 97% DMA and 92% DAAM were consumed in 90 min. GPC studies indicated $M_n = 44.2$ kg mol^{-1} and $M_w/M_n = 1.08$ of the resultant copolymer.

^1H NMR spectroscopy

^1H NMR spectra were recorded on an INOVA 400MHz NMR spectrometer at 25 °C.

Gel Permeation Chromatography (GPC)

GPC measurements were performed on a PL-GPC220 integrated system that was equipped with a refractive index detector and a set of columns consisting of two PLGel 10 μm MIXED-B columns and one PLGel 5 μm MIXED-D column. DMF containing 0.01 mol L^{-1} LiBr was used as an eluent at 80 °C at a flow rate of 1.0 mL min^{-1}. Polystyrene standards (Agilent, 3.37 ~ 6035.0 kg mol^{-1}) were used for calibration.

Dynamic light scattering (DLS)

DLS studies on thermo-responsive behaviours were performed on a Brookhaven BI-200SM setup that was fitted with a 22-mW He-Ne laser ($\lambda = 632.8$ nm), a BI-200SM goniometer and a BI-TurboCorr digital correlator. Solution temperature was adjusted using a BI-TCD controller. Typically, 10 mg P($DAAM_{52}$-*grad*-DMA_{37}) was dissolved in 10.0 mL water under stirring at 25 °C overnight. The dust was removed by passing through a 0.45 μm filter. The solution was moved to DLS sample cell, kept at 15 °C for 20 min, and then heated at a rate of 1.0 °C min^{-1} to pre-determined temperatures and then stabilized for 2 min. The light scattering intensity was collected at 90° for 5 min. The intensity-average hydrodynamic diameter (D_h) and polydispersity (μ_2/Γ^2)

of heating-induced assembly assessed using cumulants analysis using CONTIN software. The data were averaged over 3 runs.

^{1}H NMR and DLS studies on reaction-induced reorganization

Typically, P(DAAM$_{94}$-*grad*-DMA$_{113}$) (24 mg, 8.33×10^{-2} mmol of keto groups) was dissolved in 3.0 mL D_2O in 10-mL vial under stirring at 30 °C overnight. The solution of BHA (20 mg, 1.25×10^{-4} mol) and TEA (25.2 mg, 2.5×10^{-4} mol) in 3.0 mL D_2O was added in this vial. The reaction solution was stirred at 30 °C for 3 days, and then used for ^{1}H NMR and DLS studies at 20 °C.

Results and Discussion

RAFT polymerisation of DAAM monomer

As shown in scheme 1, a trithiocarbonate chain transfer agent (CTA), EDMAT, was synthesized according to the literature procedures[49] and used as a CTA. Polymerisation was initiated by TPO photo-initiator in 50 wt% methanol on irradiation with weak visible light at 25 °C.

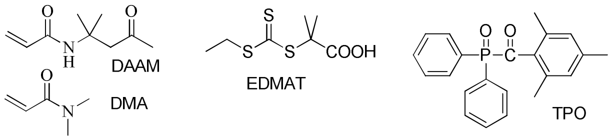

Scheme 1 Chemical structures of DAAM and DMA monomers, EDMAT chain transfer agent and TPO initiator that were selected for this study.

As shown in Fig. 1a, the polymerisations proceeded fast over a wide range of [DAAM]$_0$:[EDMAT]$_0$:[TPO]$_0$ from 50:1:0.25 to 1000:1:0.25, i.e. the targeted degrees of polymerisation, DP$_{\text{target}}$, of 50~1000, in which higher DP$_{\text{target}}$ led to faster polymerisation. Moreover, semilogarithmic kinetic curves linearly evolved with monomer conversions till 95% monomer was consumed (Fig. 1b), suggesting constant and steady contents of growing chain radicals.

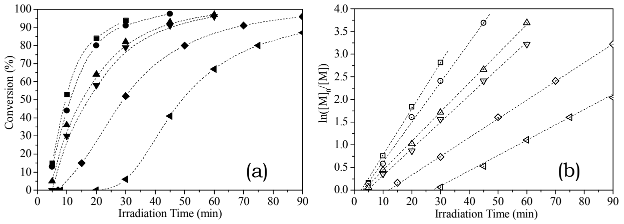

Fig. 1 Kinetic curves of RAFT polymerization of DAAM monomer at a [DAAM]$_0$:[EDMAT]$_0$:[TPO]$_0$ = 1000:1:0.25 (■), 600:1:0.25 (●), 300:1: 0.25 (▲), 200:1:0.25 (▼), 100:1:0.25 (♦) to 50:1:0.25 (◀) in 50 wt% methanol at 25 °C, on irradiation with visible light.

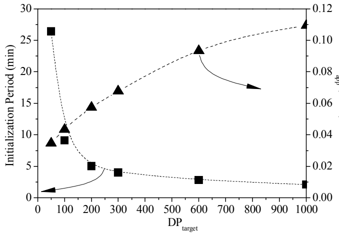

Fig. 2 Initialization periods and the apparent propagation rate constants (k_{app}) as a function of the targeted degrees of polymerization (DP$_{\text{target}}$), as assessed from Fig. 1.

As summarized in Fig. 2, RAFT initialization period[50,51] shortened remarkably from 26 to 5 min on increase of DP$_{\text{target}}$ from 50 to 200, and slightly decreased from 300 to 1000. The apparent propagation rate constants (k_{app}, the slopes of semi-logarithmic curves) increased with DP$_{\text{target}}$ up to 95% DAAM was consumed, suggesting the high efficiency of polymerisation.

As shown in Fig. 3, GPC traces are narrowed, and shift to the high molecular weight side on increasing monomer conversions. The number-average molecular weights (M_n) linearly increased with the conversions, leading to low polydispersity indices of the final polymers at M_w/M_n = 1.08 ~ 1.14. These results suggest that polymerisation was well-controlled, thus giving the well-defined keto-polymers with DPs varying widely from 50 to 1000.

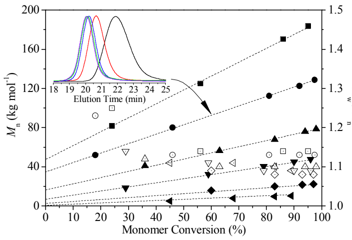

Fig. 3 Number-average molecular weight (M_n) and polydispersity index (M_w/M_n) as a function of monomer conversions on polymerisation at a [DAAM]$_0$:[EDMAT]$_0$:[TPO]$_0$ = 1000:1:0.25 (■), 600:1:0.25 (●), 300:1: 0.25 (▲), 200:1:0.25 (▼), 100:1:0.25 (♦), or 50:1:0.25 (◀). *Insert*: GPC traces of the polymers synthesized at the feed molar ratio of 600:1:0.25.

Statistical copolymerisation of DAAM and DMA

We attempted to assess reasonable reactivity ratios of this pair at relatively low conversions (e.g. < 15%,[52,53]), but unfortunately the attempts have proved ineffective because of the intrinsic initialization period in RAFT process.[50,51] Therefore, we turned to assessing the unit ratios of the copolymers that inferred from the kinetics of copolymerisation.

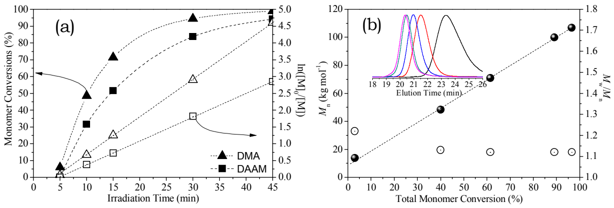

Fig. 4 (a) Kinetic curves of copolymerisation at a [DAAM]$_0$:[DMA]$_0$:[EDMAT]$_0$:[TPO]$_0$ = 300:300:1:0.25 in 50 wt% methanol on irradiation with visible light at 25 °C. (b) M_n and M_w/M_n as a function of the total monomer conversions (insert: GPC traces).

As shown in Fig. 4a, at a [DAAM]$_0$:[DMA]$_0$:[EDMAT]$_0$:[TPO]$_0$ = 300:300:1:0.25, DAAM polymerized more slowly than DMA up to 90% DAAM conversions, in which DMA was essentially consumed and GPC trace narrowed down and shifted to high molecular weight side (insert of Figure 4b), suggesting the formation of gradient copolymer. The linear increase of M_n with conversions and low polydispersity indices (Fig. 4b) suggest that well-controlled behaviour of this statistical copolymerisation.

Copolymerisation at a [DAAM]$_0$:[DMA]$_0$:[EDMAT]$_0$:[TPO]$_0$ = 100:100:1:0.25 (Electronic Supplementary Information Fig S1, Table 1) also proceeded at the same ratio of $k_{\text{app,DMA}}/k_{\text{app,DAAM}}$ as observed in the former. Moreover, the gradual variation of unit ratios in the purified copolymers with conversions (Table S1) evidenced the gradient chain-growth of copolymer. Therefore the copolymers are termed as P(DMA-*grad*-DAAM).

Cite this: DOI: 10.1039/c0xx00000x

www.rsc.org/xxxxxx

Table 1 Kinetic Parameters of RAFT Copolymerisation of DAAM and DMA Monomers in 50 wt% Methanol at 25 °C, on Irradiation with Visible Light.

feed molar ratio [a]	$T_{init,\ DMA}$ [b] (min)	$T_{init,\ DAAM}$ [b] (min)	$k_{app,\ DMA}$ [c] (min^{-1})	$k_{app,\ DAAM}$ [c] (min^{-1})	$k_{app,DMA}$ / $k_{app,DAAM}$
300:300:1:0.25	4.1	5.0	0.1129	0.0712	1.59
100:100:1:0.25	4.2	5.4	0.0697	0.0438	1.59

[a] the feed molar ratio is $[DMA]_0:[DAAM]_0:[EDMAT]_0:[TPO]_0$; [b] T_{init} is the initialization period; [c] k_{app} is the apparent propagation rate constant.

Synthesis of PDMA-*b*-PDAAM copolymer

This copolymer was synthesized *via* a two-step chain-extending copolymerisation. Firstly, DMA monomer was polymerized at a $[DMA]_0:[EDMAT]_0:[TPO]_0=120:1:0.25$ in 50 wt% methanol on irradiation with visible light at 25 °C. Secondly, as-synthesized PDMA was chain-extended by DAAM monomer at a $[DAAM]_0:[PDMA]_0:[TPO]_0=100:1:0.25$. The copolymer was assessed to be $PDMA_{113}$-*b*-$PDAAM_{93}$ according to signal *i* of EDMAT chain-ends (Fig. 5a). The clear shift of GPC trace (Fig. 5b) and the low polydispersity index of the resultant copolymer (M_w/M_n = 1.10) indicate the living character of this polymerisation.

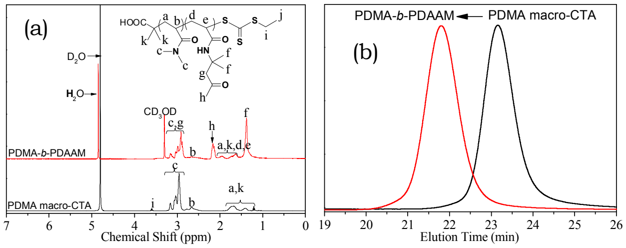

Fig. 5 (a) ^1H NMR spectra and (b) GPC traces of $PDMA_{113}$ macro-CTA and the chain-extended $PDMA_{113}$-*b*-$PDAAM_{93}$ copolymer.

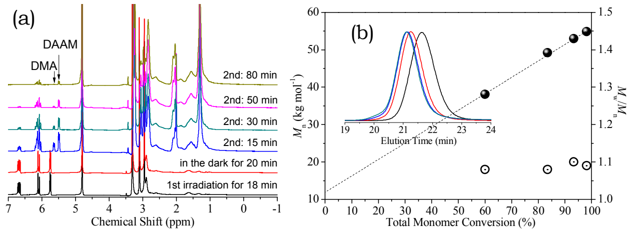

Fig. 6 (a) ^1H NMR spectrum evolution of the solution in which (from bottom to upper) the polymerisation of DMA, at a $[DMA]_0:[EDMAT]_0:[TPO]_0$ = 120:1:0.25 at 25 °C, was suspended at 31% conversion by turned off visible light. The solution kept in the dark for 20 min. Argon-gas-saturated DAAM ($[DMA]_0:[DAAM]_0$=120:100) was added in the dark, and then irradiated with visible light. (b) M_n and M_w/M_n *vs.* the total monomer conversions (insert: GPC traces).

Synthesis of PDMA-*b*-P(DAAM-*grad*-DMA) copolymer

These copolymers were synthesized *via* visible-light-mediated iterative RAFT polymerisation.[48] As shown in Fig. 6a, the water-soluble short PDMA blocks were formed on polymerisation at $[DMA]_0:[EDMAT]_0:[TPO]_0=120:1:0.25$ on irradiation for 18 min, where 31% DMA had been consumed. Moreover, the monomer conversions did not changed in between 20 min of dark period, suggesting that the reaction was suspended in the dark. Our previous results confirmed that the chain growth could restart or suspend immediately by turning on or off light,[46-48] thus leading to one-pot synthesis of copolymers with *block*, *random*, *block-random* or *block-random-block* structures.[48]

Thereafter, argon-gas-saturated DAAM solution was added in the solution in the dark, and visible light irradiation brought about copolymerisation of both monomers, as indicated by attenuation of CH_2=CHCONH signals. Similarly, DMA polymerized faster than DAAM, whose vinyl signals disappeared within 80 min but those of DAAM were still detected. As indicated by the decrease of the integrated ratio $I_{5.64}/I_{5.48}$, the ratios of unreacted monomer, [DMA]:[DAAM] lowered from 0.40, 0.11 to 0.04 on prolonging irradiation from 15, 30 to 50 min. GPC trace shifted to high molar mass side and M_n linearly increased with conversions (Fig. 6b). The results suggest well-defined PDMA-*b*-P(DAAM-*grad*-DMA).

Adding DAAM at 51% DMA conversion also led to gradient consuming of both monomers, whose unreacted monomer ratio [DMA]:[DAAM] lowered from 0.22 in 15 min, 0.05 in 30 min, to 0.01 in 50 min (Fig. S2a). Similar phenomenon was observed on adding DAAM at 75% DMA conversion, where [DMA]:[DAAM] decreased from 0.06 in 15 min to 0.03 in 30 min (Fig. S2b). These results indicate the well-defined sequence of PDMA-*b*-P(DAAM-*grad*-DMA) of these binary copolymers.

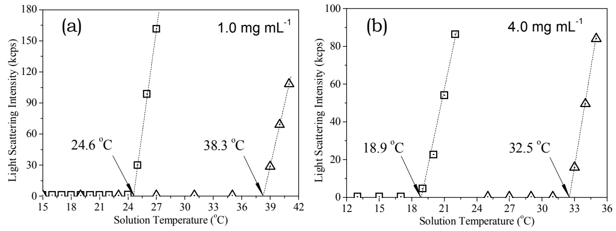

Fig. 7 The variation of the light scattering intensity of P($DAAM_{52}$-*grad*-DMA_{37}) (□) or P($DAAM_{44}$-*grad*-DMA_{46}) (Δ) in water on heating.

Temperature-tunable aqueous solubility

These properties were studied by dynamic light scattering (DLS). As shown in Fig. 7, the light scattering intensity is very low at low temperatures, suggesting that the gradient copolymers were dissolved in water. This intensity improved sharply on heating up to the critical temperatures as indicated by arrows. Thereafter, further heating led to milky solutions. This is the typical lower critical solution temperature (LCST) behaviour.[54] Therefore the critical temperatures are termed as the cloud points.

As shown in Fig. 7a, although at the same DPs and polymer concentrations (1.0 mg mL^{-1}), P($DAAM_{52}$-*grad*-DMA_{37}) had a cloud point 13.7 °C lower than P($DAAM_{44}$-*grad*-DMA_{46}) because DAAM units are more hydrophobic than DMA units. Moreover, the cloud points lowered down to ΔCP = -5.8 °C on concentrated from 1.0 to 4.0 mg mL^{-1} (Fig. 8b), suggesting that this LCST behaviour was dominated by hydrophobicity.[55,56]

As summarized in Table 2, a variety of gradient copolymers were synthesized, in which Samples 1-7 are at a DP = 90 ± 1 but the unit ratios DAAM/DMA varied from 2.33 to 0.34. Sample 8 (DP = 169, DAAM/DMA = 0.88) was utilized to illustrate the chain-length effect. Indeed, the cloud point increased from 16 °C to permanently water-soluble (e.g. > 80 °C) on varying the unit ratios from 2.33 to 0.34, similar to aldehyde-based P(PEGMA-*ran*-FPHPMA).[29] Moreover, the cloud point lowered from 43 °C (Sample 4) down to 40 °C (Sample 8) on increase DP from 91 (Sample 3) to 169 (Sample 8), similar to hydrophobicity-induced LCST behaviours of the pyrrolidone-based polymer solutions.[55,56] These results indicate the heating-triggered hydrophobic feature of these copolymers.

Table2 The structure parameters and heating-induced cloud points (CP) of P(DAAM-*grad*-DMA) copolymers at the same DPs but different compositions

No	Composition [a]	DAAM/DMA [a]	$M_{n,GPC}$ (kg mol^{-1})	M_w/M_n	CP (°C) at 1.0 mg mL^{-1}	CP (°C) at 4.0 mg mL^{-1}
1	P($DAAM_{63}$-*grad*-DMA_{27})	2.33	24.2	1.08	16.1	<15
2	P($DAAM_{52}$-*grad*-DMA_{37})	1.41	23.8	1.08	24.6	18.9
3	P($DAAM_{44}$-*grad*-DMA_{46})	0.96	23.6	1.08	38.4	32.5
4	P($DAAM_{42}$-*grad*-DMA_{49})	0.86	23.3	1.10	43.2	35.1
5	P($DAAM_{39}$-*grad*-DMA_{50})	0.78	23.3	1.10	46.8	39.2
6	P($DAAM_{34}$-*grad*-DMA_{57})	0.60	23.1	1.09	63.6	49.6
7	P($DAAM_{23}$-*grad*-DMA_{68})	0.34	22.6	1.09	>80	>80
8	P($DAAM_{79}$-*grad*-DMA_{90})	0.88	42.6	1.10	40.1	30.4

[a] The compositions and unit ratios (DAAM/DMA) of the copolymers were assessed by ^{1}H NMR.

Table 3 The structure parameters of the copolymers that were selected for the studies on the sequence regulation of thermo-responsive behaviours

No.	Composition [a]	DAAM/DMA [a]	$M_{n,\,GPC}$ (kg mol^{-1})	M_w/M_n
1	P($DAAM_{94}$-*grad*-DMA_{113})	94:113	44.4	1.12
2	$PDMA_{37}$-*b*-P($DAAM_{92}$-*grad*-DMA_{79})	92:116	44.2	1.09
3	$PDMA_{61}$-*b*-P($DAAM_{90}$-*grad*-DMA_{54})	90:115	44.0	1.11
4	$PDMA_{90}$-*b*-P($DAAM_{94}$-*grad*-DMA_{27})	94:117	44.8	1.12
5	$PDMA_{111}$-*b*-$PDAAM_{93}$	93:111	43.8	1.10

[a] the compositions and unit ratios (DAAM/DMA) of the selected copolymers were assessed by ^{1}H NMR.

Table 4 DLS results of the aqueous solutions of the copolymers (4.0 mg mL^{-1}) before and after the reaction of imine formation with BHA

Sample	State	Intensity (kcps)	D_h (nm)	Polydispersity (μ_2/Γ^2)	$D_{h,2}/D_{h,1}$ [a]
P($DAAM_{94}$-*grad*-DMA_{113})	Before	3.8	NA	NA	NA
	After	5.3	78	0.087	
$PDMA_{37}$-*b*-P($DAAM_{92}$-*grad*-DMA_{79})	Before	5.1	NA	NA	NA
	After	27.6	36	0.063	
$PDMA_{61}$-*b*-P($DAAM_{90}$-*grad*-DMA_{54})	Before	22.6	19	0.182	2.21
	After	90.6	42	0.035	
$PDMA_{90}$-*b*-P($DAAM_{94}$-*grad*-DMA_{27})	Before	36.7	15	0.156	3.2
	After	194.4	49	0.015	
$PDMA_{111}$-*b*-$PDAAM_{94}$	Before	53.0	14	0.135	4.3
	After	428.8	61	0.028	

[a] $D_{h,1}$: D_h assessed by DLS before reaction; $D_{h,2}$: D_h assessed by DLS after reaction.

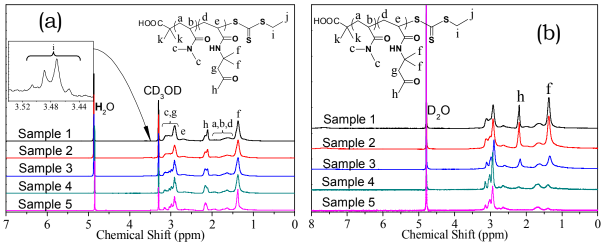

Fig. 8 ^{1}H NMR spectra of 4.0 mg mL^{-1} copolymers (Table 4) recorded in (a) methanol-d_4 or (b) deuterium oxide (D_2O) at 20 °C.

Sequence regulation on thermo-responsive behaviours

As well known, the peptide sequence determines supramolecular structures and thus the living functions of proteins. Inspired by this feature, we synthesized a range of the copolymers whose unit ratios and chain lengths are precisely controlled at DAAM/DMA of 0.81 ± 0.03 and DP of 207 ± 4 (Table 4), and the sequence was changed from *gradient*, *“short-block”-gradient*, *“middle-block”-gradient*, *“long-block”-gradient* to *block*.

As shown in Fig. 8a, signals *i* (CH_3CH_2 of EDMAT chain-ends) of the copolymers was utilized to assess the compositions and unit ratios as listed in Table 3. The symmetrical GPC traces (Figure S3) and low M_w/M_n values (1.09~1.12) suggest the narrow distributions of the copolymer samples. More importantly, as compared with those in methanol-d_4, the signals *h*, *f* of DAAM units in D_2O (Fig. 8b) are gradually attenuated on adjusting the copolymer sequence from *gradient*, *“short-block”-gradient*, *“middle-block”-gradient*, *“long-block”-gradient* to *block*. These results suggest the strong influence of sequence on dehydration of DAAM co-monomer units.

As shown in insert of Fig. 9a, Sample 1 (gradient copolymer) completely dissolved in water at relatively low temperatures, as indicated by very low light scattering intensity. The cloud point occurred at 33.5 °C, above which the solution changed to milky.

The hysteresis, which occurred on cycling the heating and cooling (see Fig. S4a), indicates the formation of the inter-chain hydrogen bonding above the cloud point.

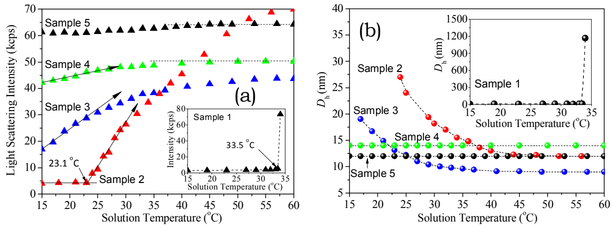

Fig. 9 The variation of (a) light scattering intensity and intensity-averaged hydrodynamic diamers (D_h) of 4.0 mg mL^{-1} of the copolymers (Table 4) in water on heating.

Sample 2 [PDMA$_{37}$-*b*-P(DAAM$_{92}$-*grad*-DMA$_{79}$)] exhibited a cloud point 10.4 °C lower than Sample 1. The formation of small particles at a D_h = 12 nm at 60 °C (Fig. 9b) suggest that the short water-soluble PDAM$_{37}$ blocks effectively stabilized the collapsed gradient blocks. The increased intensity but shrinkage of particles at elevated temperatures presumably attribute to the dehydration and formation of inter-chain hydrogen bonding as indicated by the hysteresis on cycling the heating and cooling (Fig. S4b).

Sample 3 [PDMA$_{61}$-*b*-P(DAAM$_{90}$-*grad*-DMA$_{54}$)] assembled into micelles at 15 °C. Heating from 15 to 30 °C led to the increase of light scattering intensity and the shrinkage of micelles from D_h = 19 to 10 nm, suggesting formation of compact micelles induced by dehydration. Most presumably, the hydrogen bonding of amide and ketone functionalities (in DAAM units) with water molecules enhanced chain diffusion and thus dynamic exchange, leading to miniaturization of these thermo-triggered particles.

Sample 4 [PDMA$_{90}$-*b*-P(DAAM$_{94}$-*grad*-DMA$_{27}$)] organized to compact micelles at 15 °C, which exhibited heating-induced shrinkage similar to PDMA$_{111}$-*b*-PDAAM$_{93}$ micelles but slightly larger than the latter. The results suggest that the strong influence of copolymer sequence on the heating-induced assembly and swelling-shrinking behaviours.

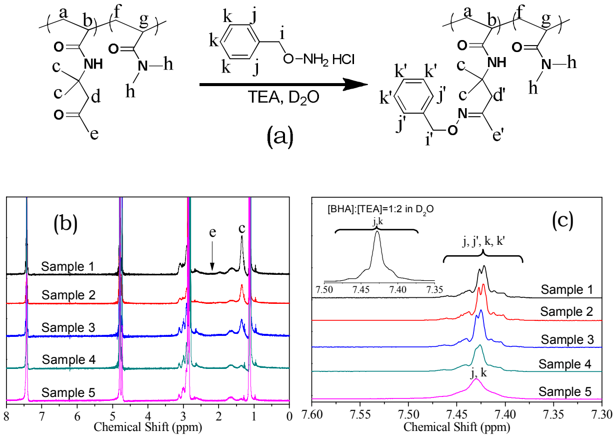

Fig. 10 (a) The reaction of polymeric keto groups with BHA; (b) ^{1}H NMR spectra of 4.0 mg mL^{-1} copolymers (see Table 3) in D_2O after reaction at a $[DAAM]_0$:$[BHA]_0$:$[TEA]_0$ = 1:1.5:3.0 at 20 °C for 3 days; (c) ^{1}H NMR spectra of the benzene rings in the BHA-conjugated copolymer solutions.

Reorganization induced by the reaction of ketone groups

As shown in Fig. 10a, O-benzylhydroxylamine hydrochloride (BHA) was employed because of reasonably high reactivity with the polymeric ketone groups.[45] This reaction proceeded at a $[DAAM]_0$:$[BHA]_0$:$[TEA]_0$ = 1:1.5:3.0 in D_2O at 20 °C for 3 days. Triethylamine (TEA) was added to convert the acidified oxime groups into the neutralized forms.

As shown in Fig. 10b, signal *e* (CH_3(C=O)CH_2 in DAAM units) disappeared even in Sample 1 (the gradient copolymer), suggesting that DAAM co-units was fully conjugated with BHA. However, signal *c* (CONHC(CH_3) in DAAM units) of Samples 1-3 was detected, which were quite similar to those observed before reaction (Fig. 8b). These results demonstrate that neighbouring amide spacers enhanced hydration of DAAM units. Moreover, as compared with signals *j*, *k* of the neutralized BHA (insert of Fig. 10c), the signals *j'*, *k'* (benzene rings of the reacted BHA residues) of Sample 1 could be detected, but which were attenuated and undetectable on adjusted the sequence from *block-gradient* to *block*. The results suggest that the hydration behaviours of BHA-conjugated DAAM units could be effectively tuned by adjusting the comonomer sequence.

As shown in Table 4, the light scattering intensity increased on conjugation with BHA, leading to assembly of water-soluble gradient and "short-block"-gradient copolymers. Moreover, the dispersity narrowed down to μ_2/Γ^2 = 0.087~ 0.028, suggesting that conjugation of BHA induced the dynamic rearrangement of polymer chains. The micelles were enlarged in the order of *block* > *"long-block"-gradient*>*"middle-block"-gradient*>*"short-block"-gradient* > *gradient*, as indicated by the size ratio of $D_{h,2}/D_{h,1}$. The results demonstrate that the strong effect of the sequence on the reaction-induced dynamic reorganization.

Conclusions

Facile synthesis, sequence-tuned thermo-responsive behaviours, reaction-induced reorganization of water-soluble keto-polymers were reported in this paper. To this end, a commercially-available DAAM monomer was polymerized *via* RAFT polymerisation in methanol on irradiation with visible light at 25 °C. The statistical copolymerisation with DMA monomer proceeded under identical conditions. The copolymers with tailored structures of PDMA-*b*-P(DAAM-*grad*-DMA) were also synthesized *via* one-pot iterative process. The effect of the copolymer sequence on the dehydration, heating-triggered phase transition, assembly and reaction-induced dynamic reorganization were studied by ^{1}H NMR, GPC and DLS.

The results demonstrated that the polymerisation of DAAM was well-controlled, leading to the well-defined DAAM homo-polymers over a wide range of DPs over 50 ~ 1000 and diblock copolymer with PDMA. Statistical copolymerisation with DMA gave gradient-distributed P(DAAM-*grad*-DMA), whose aqueous solubility could be finely tuned. The binary copolymers having the tailored structures of PDMA-*b*-P(DAAM-*grad*-DMA) were also synthesized *via* one-pot iterative process. P(DAAM-*grad*-DMA) exhibited typical thermoresponsive behaviours on heating, whose cloud point could be tuned from 16 °C to permanently water-soluble. Adjusting sequence from *gradient*, *"short-block"-gradient*, *"middle-block"-gradient*, *"long-block"-gradient* to *block* effectively induced the diversity in dehydration, heating-triggered phase transition, self-assembly and reaction-induced dynamic reorganization. The well-defined water-soluble reactive keto-polymers are promising for emerging biological applications on demand in physiological aqueous solution.

ACKNOWLEDGMENT. We thank National Natural Science Foundation of China (21274097, 21334004) and the Priority Academic Program Development of Jiangsu Higher Education Institutions for financial support of this work. Mr. Zhaolan Chen, general manager of Hipro Polymer Materials Co., is also thanked for his kind offer of the research fund.

Notes and references

Jiangsu Key Laboratory of Advanced Functional Polymer Design and Application, College of Chemistry, Chemical Engineering and Materials Science, Soochow University, Suzhou 215123, China. Tel (Fax): +86-512-65884419; E-mail: ylcai@suda.edu.cn

† Electronic Supplementary Information (ESI) available: kinetics of co-polymerisation at [DAAM]$_0$:[DMA]$_0$:[EDMAT]$_0$:[TPO]$_0$=100:100:1:0.25, M_n and M_w/M_n values vs. conversions, GPC traces of copolymers (Table 4), variation of light scattering intensity in cycling the heating and cooling. See DOI: 10.1039/b000000x/

1 K. A. Günay, P. Theato, H.-A. Klok, *J. Polym. Sci., Part A: Polym. Chem.,* 2013, **51**, 1.

2 P. A. Woodfield, Y. Zhu, Y. Pei, P. J. Roth, *Macromolecules,* ASAP, DOI: 10.1021/ma402391a.

3 X. Wu, H. Zhao, B. Nörnberg, P. Theato, G. A. Luinstra, *Macromolecules,* ASAP, DOI: 10.1021/ma401899h.

4 P. Yang, L. P. D. Ratcliffe, S. P. Armes, *Macromolecules,* 2013, **46**, 8545.

5 J. Y. Quek, Y. Zhu, P. J. Roth, T. P. Davis, A. B. Lowe, *Macromolecules,* 2013, **46**, 7290.

6 H. Mori, E. Kudo, Y. Saito, A. Onuma, M. Morishima, *Macromolecules,* 2010, **43**, 7021.

7 K. Nakabayashi, S. Inoue, Y. Abiko, H. Mori, *Macromolecules,* 2013, **46**, 4790.

8 X. Ji, J. Chen, X. Chi, F. Huang, *ACS Macro Lett.,* 2014, **3**, 110.

9 K. Nakabayashi, H. Oya, H. Mori, *Macromolecules,* 2012, **45**, 3197.

10 C. B. Nielsen, R. S. Ashraf, S. Rossbauer, T. Anthopoulos, I. McCulloch, *Macromolecules,* 2013, **46**, 7727.

11 S.-M. Lee, S. T. Nguyen, *Macromolecules,* 2013, **46**, 9169.

12 S. Taskin, B. Kiskan, Y. Yagci, *Macromolecules*, 2013, **46**, 8773.

13 K. Nakabayashi, Y. Abiko, H. Mori, *Macromolecules*, 2013, **46**, 5998.

14 H. Zhao, W. Gu, M. W. Thielke, E. Sterner, T. Tsai, T. P. Russell, E. B. Coughlin, P. Theato, *Macromolecules*, 2013, **46**, 5195.

15 R. Duncan, *Nat. Rev. Cancer*, 2006, **6**, 688.

16 S. Deshayes, H. Cabral, T. Ishii, Y. Miura, S. Kobayashi, T. Yamashita, A. Matsumoto, Y. Miyahara, N. Nishiyama, K. Kataoka, *J. Am. Chem. Soc.* 2013, **135**, 15501.

17 D. C. Tully, M. J. Roberts, B. H. Geierstanger, R. B. Grubbs, *Macromolecules* 2003, **36**, 4302.

18 R. C. Li, J. Hwang, H. D. Maynard, *Chem. Commun.* 2007, **43**, 3631.

19 N. A. A. Rossi, Y. Zou, M. D. Scott, J. N. Kizhakkedathu, *Macromolecules* 2008, **41**, 5272.

20 J. M. Stukel, R. C. Li, H. D. Maynard, M. R. Caplan, *Biomacromolecules*, 2010, **11**, 160.

21 G. Sun, C. Cheng, K. L. Wooley, *Macromolecules*, 2007, **40**, 793.

22 M. Shi, A.-L. Li, H. Liang, J. Lu, *Macromolecules,* 2007, **40**, 1891.

23 N. Xiao, A. Li, H. Liang, J. Lu, *Macromolecules,* 2008, **41**, 2374.

24 G. Sun, H. Fang, C. Cheng, P. Lu, K. Zhang, A. V. Walker, J.-S. A. Taylor, K. L. Wooley, *ACS Nano,* 2009, **3**, 673.

25 B. S. Murray, A. W. Jackson, C. S. Mahon, D. A. Fulton, *Chem. Commun.,* 2010, **46**, 8651.

26 C. Cao, K. Yang, F. Wu, X. Wei, L. Lu, Y. Cai, *Macromolecules*, 2010, **43**, 9511.

27 K. Yang, X. Wei, F. Wu, C. Cao, J. Deng, Y. Cai, *Soft Matter*, 2011, **7**, 5861.

28 Z. Hao, G. Li, K. Yang, Y. Cai, *Macromol. Rapid Commun.*, 2013, **34**, 411.

29 F. Wu, X. Tang, L. Guo, K. Yang, Y. Cai, *Soft Matter,* 2013, **9**, 4036.

30 J. Deng, Y. Cai, *Macromol. Rapid Commun.*, 2013, **34**, 1459.

31 J. Chiefari, Y. K. B. Chong, F. Ercole, J. Krstina, J. Jeffery, T. P. T. Le, R. T. A. Mayadunne, G. F. Meijs, C. L. Moad, G. Moad, E. Rizzardo, S. H. Thang, *Macromolecules,* 1998, **31**, 5559.

32 N. Venkatesan, B. H. Kim, *Chem. Rev.,* 2006, **106**, 3712.

33 R. E. Kieltyka, M. M. C. Bastings, G. C. van Almen, P. Besenius, E. W. L. Kemps, P. Y. W. Dankers, *Chem. Commun.*, 2012, **48**, 1452.

34 B. M. Lamb, S. Park, M. N. Yousaf, *Langmuir*, 2010, **26**, 12817.

35 D. Dutta, A. Pulsipher, W. Luo, H. Mak, M. N. Yousaf, *Bioconjugate Chem.,* 2011, **22**, 2423.

36 M. Langer, F. Kratz, B. Rothen-Rutishauser, H. Wunderli-Allenspach, A. G. Beck-Sickinger, *J. Med. Chem.*, 2001, **44**, 1341.

37 L. Yi, Y. Chen, Lin, P.; H. Schröder, C. M. Niemeyer, Y. Wu, R. S. Goody, G. Triola, H. Waldmann, *Chem. Commun.,* 2012, **48**, 10829.

38 L. S. Witus, C. Netirojjanakul, K. S. Palla, E. M. Muehl, C.-H. Weng, A. T. Iavarone, M. B. Francis, *J. Am. Chem. Soc.,* 2013, **135**, 17223.

39 Y. Chen, G. Triola, H. Waldmann, *Acc. Chem. Res.*, 2011, **44**, 762.

40 K. J. Mackenzie, M. B. Francis, *J. Am. Chem. Soc.*, 2013, **135**, 293.

41 D. G. Barrett, M. N. Yousaf, *Biomacromolecules,* 2008, **9**, 2029.

42 C. M. Schilli, A. H. E. Müller, E. Rizzardo, S. H. Thang, Y. K. Chong, *ACS Symposium Series*, 2003, **854**, 603.

43 T. Krasia, R. Soula, H. G. Börner, H. Schlaad, *Chem. Commun.*, 2003, 538.

44 S. Bandyopadhyay, X. Xia, A. Maiseiyeu, G. Mihai, S. Rajagopalan, D. Bong, *Macromolecules*, 2012, **45**, 6766.

45 J. Liu, R. C. Li, G. J. Sand, V. Bulmus, T. P. Davis, H. D. Maynard, *Macromolecules*, 2013, **46**, 8.

46 Y. Shi, G. Liu, H. Gao, L. Lu, Y. Cai, *Macromolecules*, 2009, 42, 3917.

47 G. Liu, H. Shi, Y. Cui, J. Tong, Y. Zhao, D. Wang, Y. Cai, *Polym. Chem.*, 2013, **4**, 1176.

48 J. Tong, Y. Shi, G. Liu, T. Huang, N. Xu, Z. Zhu, Y. Cai, *Macromol. Rapid Commun.*, 2013, **34**, 1827.

49 A. J. Convertine, B. S. Lokitz, Y. Vasileva, L. J. Myrick, C. W. Scales, A. B. Lowe, C. L. McCormick, *Macromolecules*, 2006, **39**, 1724.

50 J. B. McLeary, J. M. McKenzie, M. P. Tonge, R. D. Sanderson, B. Klumperman, *Chem. Commun.,* 2004, **40**, 1950.

51 J. B. McLeary, F. M. Calitz, J. M. McKenzie, M. P. Tonge, R. D. Sanderson, B. Klumperman, *Macromolecules*, 2004, **37**, 2383.

52 J. P. Kennedy, T. Kelen, F. Tüdos, *J. Polym. Sci., Polym. Chem. Ed.,* 1975, **13**, 2277.

53 F. Ziaee, M. Nekoomanesh, *Polymer*, 1998, **39**, 203.

54 C. Weber, R. Hoogenboom, U. S. Schubert, *Prog. Polym. Sci.,* 2012, **37**, 686.

55 J. Deng, Y. Shi, W. Jiang, Y. Peng, L. Lu, Y. Cai, *Macromolecules*, 2008, **41**, 3007.

56 J. Sun, Y. Peng, Y. Chen, Y. Liu, J. Deng, L. Lu, Y. Cai, *Macromolecules*, 2010, **43**, 4041.

For Table of Contents Entry Use Only

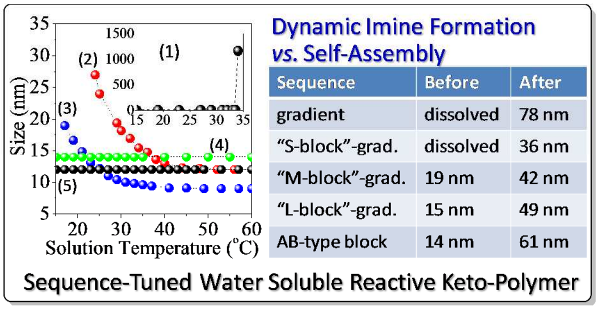

Sequence	Before	After
gradient	dissolved	78 nm
“S-block”-grad.	dissolved	36 nm
“M-block”-grad.	19 nm	42 nm
“L-block”-grad.	15 nm	49 nm
AB-type block	14 nm	61 nm

Water-Soluble Keto-Polymers: facile synthesis in methanol on irradiation with visible light at 25 °C, sequence-tuned thermoresponsive behaviours and reaction-induced reorganization